Diastereoisomer Interconversion in Chiral BiphepPtX_2 Complexes

Melanie D. Tudor, Jennifer J. Becker, Peter S. White, and Michel R. Gagné*

Department of Chemistry CB#3290, University of North Carolina, Chapel Hill, North Carolina 27599-3290

Received July 20, 2000

Reaction of biphepPt(CO_3) (biphep = 2,2′-bis(diphenylphosphino)-1,1′-biphenyl) with BINOL or HN(Tf)CHPhCHPhOH (TfNO) yielded square-planar biphepPtX_2 (X_2 = BINOL, N(Tf)CHPhCHPhO) complexes as a mixture of diastereomers (∼1:1). BiphepPtCl_2 also reacted with Na_2BINOL to generate biphepPt(BINOL) as a 1:1 mixture of diastereomers. With racemic BINOL or TfNO ligands, the mixtures were prone to isomerize to thermodynamic diastereomer mixtures (BINOL, 95:5; TfNO, >97:3) by an X_2−X_2 ligand−ligand exchange mechanism that was rapid at room temperature. With enantiopure ligands the X_2−X_2 ligand−ligand exchange process was degenerate and nonproductive. However, thermolysis of 1:1 mixtures of enantiopure biphepPt(BINOL) diastereomers (92−122 °C) cleanly established thermodynamic equilibrium by a process that involves biphenyl atropisomerism ($\Delta H^{\ddagger} = 27(2)$ kcal mol^{-1}, $\Delta S^{\ddagger} = -5(5)$ eu). Two mechanisms for this process were considered, concerted stereoinversion via a planar seven-membered metallacycle, and one-arm-off prior to a biphenyl isomerization (anti disposed PPh_2 units). In pyridine, a third mechanism for atropisomerism was identified and proposed to involve a five-coordinate pyridine intermediate (not observed) with an enhanced phosphine dissociation rate. Pyridine lowered the isomerization temperature of enantiopure complexes by ∼50 °C. X-ray structures of the thermodynamically favored biphepPt(TfNO) ((±)-**4a**) and the thermodynamically less favored biphepPt(BINOL) ($\lambda(S)$-**5b**) diastereomers were obtained, and a stereochemical model to explain the diastereoselectivity was formulated.

Introduction

What is the mechanism by which 2,2′-bis(diphenylphosphino)biphenyl (biphep) interconverts its chiral skew conformations when coordinated to a transition metal fragment? We pose this question in the context of recent clever experiments that take advantage of a chiral metal fragment's ability to affect the population of biphep conformations and thereby access selective catalysts for the asymmetric transfer hydrogenation of ketones.[1] These experiments in effect trick biphep into acting like BINAP, the well-known and highly selective diphosphine ligand. This despite the fact that biaryl rotation in free biphep is too fast for enantiomer resolution ($\Delta G^{\ddagger} = 22 \pm 1$ kcal mol^{-1}, 125 °C).[2]

In the Mikami/Noyori experiment, addition of enantiopure 1,2-diphenylethylenediamine to biphep$RuCl_2$-$(dmf)_n$ quickly generates a 1:1 mixture of diastereomers that is stable in $CDCl_3$, but that relaxes to a 3:1 mixture with a half-life in the 10's of seconds in 1:2 $CDCl_3$/$(CD_3)_2$-CDOD (eq 1). All data point to biaryl rotation being the key step in the atrop-interconversion and at rates consistent with the rotational barrier measured in the free ligand. Simple on-metal atrop-inversion and one-arm-off prior to biaryl rotation were proposed as reasonable mechanisms for the equilibration of the diastereomers.

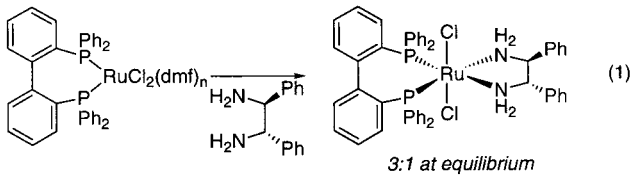

(1)

3:1 at equilibrium

To gain insight into the mechanism of diastereomer interconversion and to specifically address the issue of on-metal ligand twisting versus arm-off (free ligand-like) mechanisms for atrop isomer inversion, we have examined the isomerization of substitution-inert chiral biphepPtX_2 complexes, where X_2 is BINOL or a chelating O,NTf ligand. Unlike octahedral Ru(II) complexes, square-planar Pt(II) complexes generally react via associative mechanisms. We rationalized that this distinction would enable one-arm-off and on-metal inversion processes to be distinguished (both intramolecular processes). Moreover, chiral P_2PtX_2 complexes would also distinguish and rank the relative importance of competing ligand exchange (no biaryl rotation, an intermolecular isomerization) and atrop-inversion mechanisms for diastereomer equilibration (e.g., Scheme 1). Though the products from the intra- and intermolecular isomerization are enantiomeric, we loosely refer to both processes as "isomerization" mechanisms.

Results and Discussion

(1) Ligand and Precursor Synthesis. Given the capricious nature of the known methods for synthesizing

(1) Mikami, K.; Korenaga, T.; Terada, M.; Ohkuma, T.; Pham, T.; Noyori, R. *Angew. Chem., Int. Ed.* **1999**, *38*, 495−497.
(2) Desponds, O.; Schlosser, M. *Tetrahedron Lett.* **1996**, *37*, 47−48.

10.1021/om000629a CCC: $19.00
Publication on Web 09/22/2000

Scheme 1

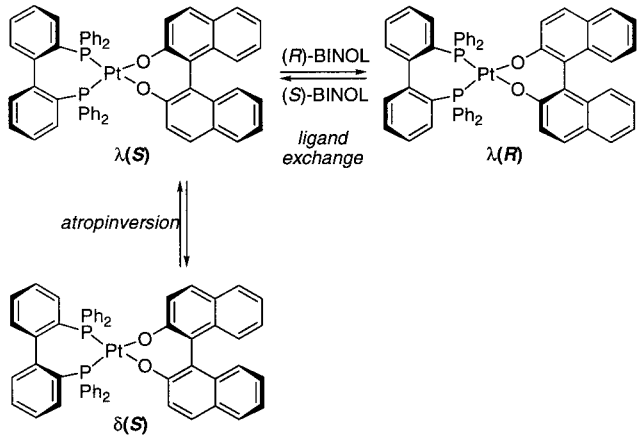

the biphep ligand,[2,3] we have examined several alternative syntheses of this ligand. First explored was the oxidative coupling of the monoanion obtained by the lithiation of Ph_3PO with sec-BuLi in THF (−78 °C) (eq 2). Adding this deep orange solution to a bright blue

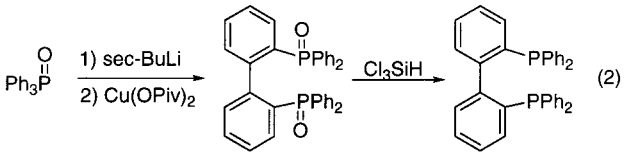

solution of $Cu(OPiv)_2$ (0 °C) yielded the coupled diphosphine oxide ligand. This Cu(II)-based methodology is superior to the copper bronze-mediated Ullman coupling of 2-iodotriphenylphosphine oxide, as it reduces the number of synthetic steps from 2 to 1 and the time to multigram quantities of ligand from Ph_3PO to 2 days from 1 week. The crude biphep oxide was then reduced with Cl_3SiH in refluxing xylene to yield the desired ligand contaminated with unreacted PPh_3. Biphep was obtained in 30% overall yield after a single recrystallization from toluene/ethanol. Two alternative procedures based on the $(dppe)NiCl_2$-catalyzed coupling of $ClPPh_2$[4] or $HPPh_2$[5] with the ditriflate of 2,2′-biphenol were found to directly yield biphep, but unidentified byproducts and long reaction times made these approaches less amenable to scale-up. During the preparation of this article Hayashi reported a $Pd(OAc)_2$/dppb-catalyzed procedure for coupling the ditriflate of 2,2′-biphenol with $HPPh_2O$ in high yields that is amenable to scale-up.[6]

The reaction of biphep with $(COD)PtCl_2$ was straightforward and provided biphep$PtCl_2$, **1**, which was recrystallized from CH_2Cl_2/MeOH (eq 3). The desired biphep$Pt(CO_3)$, **2**, could be readily generated from the dichloride and Ag_2CO_3 in wet CH_2Cl_2 by the procedure of Andrews.[7] Like **1**, the carbonate was soluble in CH_2Cl_2 and was completely characterized. Phosphorus chemical

Table 1. ^{31}P Chemical Shift and Coupling Constants for Selected Complexes (CD_2Cl_2)

complex	^{31}P chemical shift (ppm)	J_{P-Pt} (J_{P-P}) (Hz)
1	7.9	3610
2	2.2	3570
4a (major)	7.2	3760 (31.3)
	3.5	3210 (31.3)
4b (minor)	8.9	3725 (32.3)
	4.8	3210 (32.3)
5a (major)	2.9	3670
5b (minor)	2.6	3643

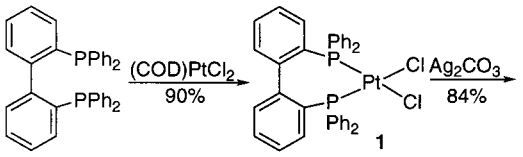

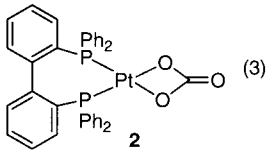

shifts and J_{P-Pt} values are collected in Table 1 for all reported complexes.

(2) Synthesis of BiphepPtX$_2$ Complexes. The reaction of **2** with 0.9 equiv of (±)-**3** in CD_2Cl_2 yielded the desired product after 1 h as a ∼1:1 ratio of diastereomers, (±)-**4a** and (±)-**4b** (eq 4), along with traces of **1** and **2**. The isomer ratio remained constant in solution

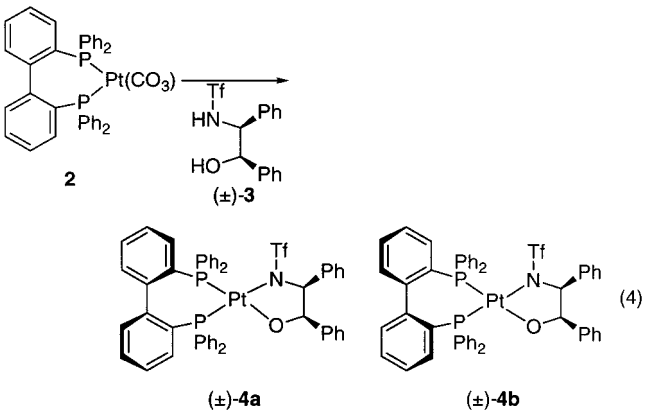

over 3 days at ambient temperature provided that traces of **2** were present. The reduced rate of λ- and δ-skew interconversion in biphep (cf. dppe)[8] is consistent with the observation of two diastereomers in the ^{31}P NMR; at a minimum the biphep δ/λ interconversion is slow on the NMR time scale. Consistent with our previous characterization of dppePtNO complexes,[8] we assign the upfield set of doublets (3.5 and 4.8 ppm) to the phosphines in (±)-**4a** and (±)-**4b** that are trans to the alkoxide (J_{Pt-P} typically 3200−3250 Hz) and the downfield resonances (7.2 and 8.9 ppm) to those trans to the triflamide (J_{Pt-P} typically 3600−3700 Hz), Table 1. The 1:1 ratio of enantiopure diastereomers, λ(1*R*,2*S*)-**4a** and δ(1*R*,2*S*)-**4b**, was invariant and the mixture could be isolated using 1 equiv of (1*R*,2*S*)-**3** (eq 5) in 40% yield after recrystallizing from CH_2Cl_2/hexanes.

(3) Desponds, O.; Schlosser, M. *J. Organomet. Chem.* **1996**, *507*, 257−261.
(4) Ager, D. J.; East, M. B.; Eisenstadt, A.; Laneman, S. A. *Chem. Commun.* **1997**, 2359−2360.
(5) Cai, D.; Payack, J. F.; Bender, D. R.; Hughes, D. L.; Verhoeven, T. R.; Reider, P. J. *J. Org. Chem.* **1994**, *59*, 7180−7181.
(6) Ogasawara, M.; Yoshida, K.; Hayashi, T. *Organometallics* **2000**, *19*, 1567−1571.
(7) Andrews, M. A.; Gould, G. L.; Klooster, W. T.; Koenig, K. S.; Voss, E. J. *Inorg. Chem.* **1996**, *35*, 5478−5483.
(8) Becker, J. J.; White, P. S.; Gagné, M. R. *Inorg. Chem.* **1999**, *38*, 798−801.

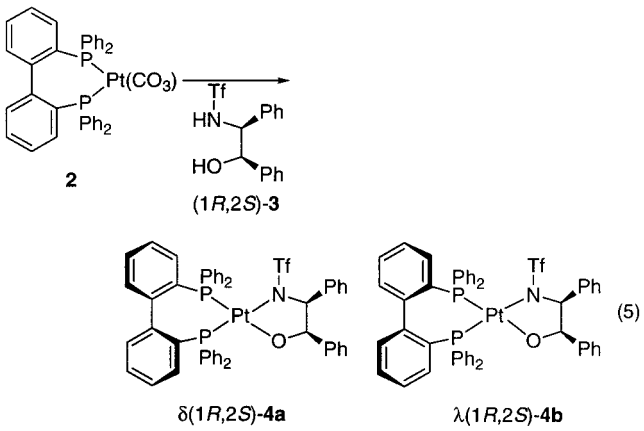

A nearly 1:1 ratio of biphepPt(BINOL) diastereomers was obtained by a salt elimination protocol that relied on a soluble source of Na_2BINOL obtained from in situ deprotonation of BINOL with NaOtBu[9] (eq 6). In

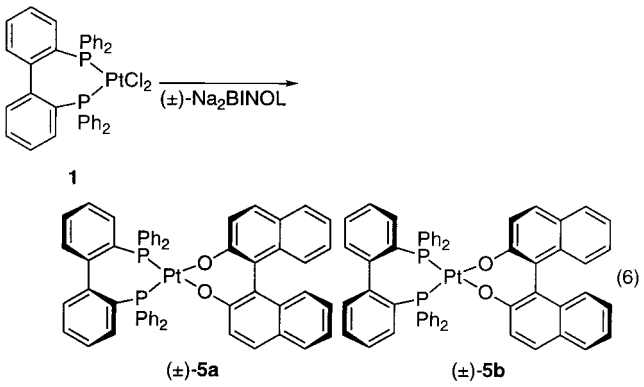

toluene, NaCl elimination from (±)-Na_2BINOL·tBuOH$_x$ and biphepPtCl_2 is complete within 30 min, and the BINOLate diastereomers ((±)-**5a** and (±)-**5b**) are obtained in 82% yield after filtration in CH_2Cl_2; ^{31}P chemical shifts and J_{Pt-P} coupling constants are compiled in Table 1. Enantiopure mixtures of these diastereomers were obtained by an analogous procedure using (*S*)-Na_2BINOL and biphepPtCl_2, or from **2** and (*S*)-BINOL (eq 7). The thermodynamically less preferred

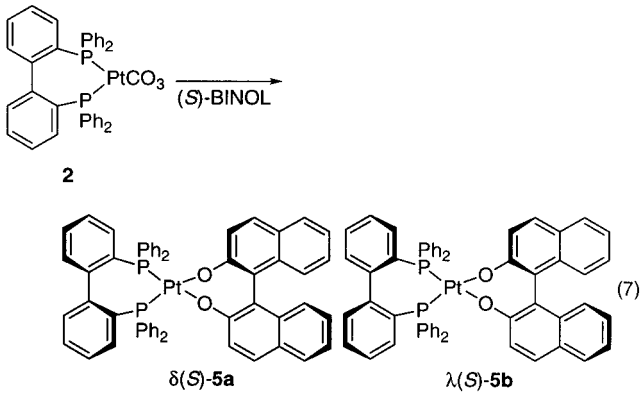

isomer (λ(*S*)-**5b**, vide infra) can be obtained in pure form (33% yield, 50% max) by fractional precipitation from toluene/hexane. Recrystallization from CH_2Cl_2 provided a single crystal of λ(*S*)-**5b**, which is described in detail in section 5. Dissolving a portion of the X-ray crystals confirmed (^{31}P NMR) that the crystals contained only the minor isomer, and thus the structure corresponded to λ(*S*)-**5b**.

(3) Influence of Added X_2 Ligands on Diastereomer Interconversion. Since one mechanism for diastereomer interconversion in chiral biphep complexes is exchange of the chiral X_2 ligand for one of opposite absolute stereochemistry (no biaryl rotation, Scheme 1), we undertook a series of NMR experiments wherein like and unlike ligands were added to the ~1:1 mixture of racemic and enantiopure diastereomers obtained in section 2.

Addition of 0.2 equiv of (±)-**3** to a mixture of (±)-**4a** and (±)-**4b** that was otherwise stable to isomerization in an NMR tube at room temperature caused one of the diastereomers to slowly increase at the expense of the other. After 12 h, the diastereomer that was characterized by the upfield set of two resonances was undetectable by ^{31}P NMR; the major isomer (**4a**, vide infra) is highly favored (>97:3) at equilibrium. Thus, the ratio of the racemates **4a**/**4b** is only constant in the absence of excess ligand, and 0.9 equiv (or less) of **3** was utilized to make a 1:1 mixture of diastereomers. A single diastereomer of (±)-**4a** was obtained as indicated in eq 4, except with 1.1 equiv of (±)-**3** and overnight gentle heating. X-ray quality crystals of (±)-**4a** were obtained by slow diffusion of Et_2O into a CH_2Cl_2 solution (see section 5).[10] Similarly, addition of 20 mol % of (±)-BINOL to (±)-**5a**/**5b** led to the rapid conversion of the mixture to one major isomer in a ~95:5 ratio, as determined by ^{31}P NMR. The major isomer of biphepPt(BINOL) was normally obtained by combining (±)-BINOL and **2** in CH_2Cl_2, which leads to the slow precipitation of the major isomer from solution. Since the kinetic diastereoselectivity is known to be low from experiments with (*S*)-BINOL (section 2), the diastereomers must isomerize rapidly upon formation. These experiments demonstrate that excess ligand catalyzes diastereomer exchange by enabling ligand−ligand exchange to match the biphep and X_2 ligand stereochemistries.

Unlike the above examples, addition of (1*R*,2*S*)-**3** and (*S*)-BINOL to the enantiopure mixtures of δ(1*R*,2*S*)-**4a**, λ(1*R*,2*S*)-**4b**, and δ(*S*)-**5a**, λ(*S*)-**5b**, respectively, did not change the ratio of diastereomers, even after overnight heating at 70 °C in toluene. On the other hand, 1 equiv of the opposite ligand enantiomers, (1*S*,2*R*)-**3** (eq 8) and (*R*)-BINOL (eq 9), respectively, led to isomerization and thermodynamic product ratios. Figure 1 shows a reversible first-order treatment[11] of the conversion of λ(*S*)-**5b** to the major diastereomer (λ(*R*)-**5a**) by the action of 1 equiv of (*R*)-BINOL at 45 °C, as monitored by ^{31}P NMR[12]

(9) The salt can be generated in either THF or toluene with a trace of THF. The presence of tBuOH is apparently important to solubility, as the pure salt is only sparingly soluble in THF once the tBuOH has been removed in vacuo.

(10) Dissolving the X-ray crystals confirmed that it was the major diastereomer that crystallized.

(11) The integrated rate expression for a standard reversible first-order process (**A** ↔ **B**) is

$$\frac{[B]_{eq}}{[A]_0} \ln \frac{[B]_{eq}}{[B]_{eq} - [B]_t} = kt$$

Plotting the left-hand side of the expression versus time yields a line with a slope of *k*, the forward rate constant. Laidler, K. J. *Chemical Kinetics*, 3rd ed.; Harper & Row: New York, 1987.

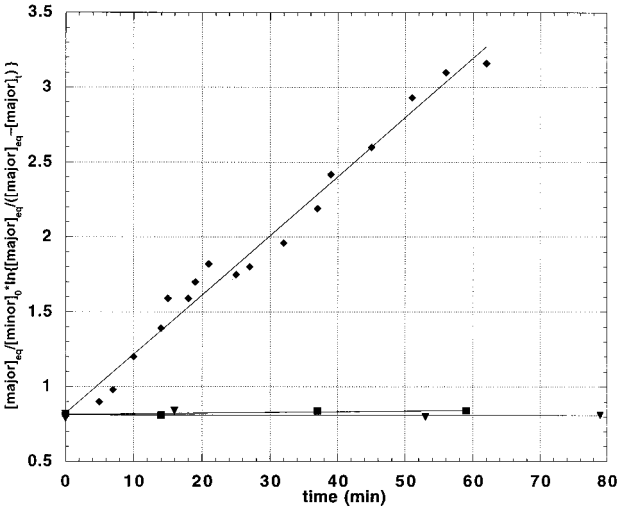

Figure 1. Reversible first-order treatment for the conversion of $\lambda(S)$-**5b** to $\lambda(R)$-**5a** (eq 9, see ref 11) with 1 equiv of (*R*)-BINOL at 45 °C in chlorobenzene. The flat lines are controls with 1 equiv of (*S*)-BINOL and no additive. $[\text{minor}]_0 = 15.0$ mM; $[\text{major}]_{t=0} = 8.2$ mM; $[\text{minor}]_{eq} = 0.9$ mM; and $[\text{major}]_{eq} = 14.1$ mM.

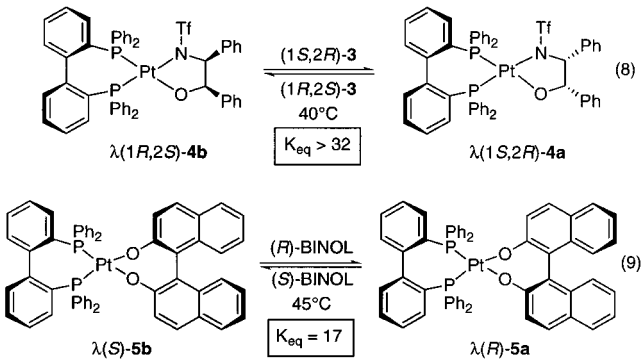

($k = 6.6 \times 10^{-4}$ s^{-1}, $\Delta G^{\ddagger} = 23$ kcal mol^{-1}, 94.4:5.6 at equilibrium). Since the minor triflamide diastereomer is not observed at equilibrium, an irreversible first-order rate treatment was utilized; $k = 3.4 \times 10^{-4}$ s^{-1} (35 °C, $\Delta G^{\ddagger} = 23$ kcal mol^{-1}) for minor to major (eq 8).

When 1 equiv of (*R*)-BINOL is used to isomerize the enantiopure diastereomers, the equilibrium ratio of (*R*)- and (*S*)-BINOL is 1, and the equilibrium constant for eq 9 can be directly determined from the ratio of diastereomers. K_{eq} is thus 16.9 at 45 °C for biphepPt(BINOL) and >32 for biphepPt(ONTf) at 35 °C.

These experiments indicate that BINOL and **3** provide a strong thermodynamic preference for a single biphep skew conformation. Furthermore, these data are most consistent with a diastereomer interconversion mechanism that is not biphep inversion, but simple ligand−ligand exchange.

(4) Thermolysis of Diastereomer Mixtures. Although ligand−ligand exchange dominates when both enantiomers of the chiral ligands are available, the question of biaryl inversion in the absence of added ligand remained unanswered. The enantiopure diastereomer mixtures were thermolyzed to determine if other isomerization mechanisms were operative.[13] Heating a ~1:1 mixture of $\delta(1R,2S)$-**4a** and $\lambda(1R,2S)$-**4b** in toluene-d_8 to 100 °C, with or without added (1*R*,2*S*)-**3**, caused the minor isomer to disappear, though extensive decomposition masked whether the minor isomer was converting to the major or it was decomposing. Since the major diastereomer, (±)-**4a** (>97:3), did not decompose at 100 °C, this suggested that the minor diastereomer either decomposed before or competitive with isomerization.

On the other hand, heating a chlorobenzene solution of $\lambda(S)$-**5b** to elevated temperature (92−122 °C) cleanly converted it to the major isomer (~94:6). Rate data obtained by ^{31}P NMR indicated that the process obeyed standard first-order relaxation to equilibrium kinetics. First-order rate constants for the minor to major conversion and equilibrium ratios are collected in Table 2. Eyring analysis of rate data obtained over a ~30 °C temperature range yielded $\Delta H^{\ddagger}$ and $\Delta S^{\ddagger}$ of 27(2) kcal mol^{-1} and −5(5) eu, respectively (Figure 2).[14] A van't Hoff analysis of the equilibrium data obtained from the thermolysis experiments provided $\Delta H° = -2.2(4)$ kcal mol^{-1} and $\Delta S° = -0.6(10)$ eu for the reaction.

(5) Structural Rationale for the Thermodynamic Selectivity. To provide a structural rationale for the

Table 2. Rate and Equilibrium Data for the Thermal Conversion of $\lambda(S)$-5b to $\delta(S)$-5a

temp (°C)	k (s^{-1})	equilibrium (major:minor)	K_{eq}
45[a]		94.4:5.6	16.9(5)
92.6	2.3×10^{-5}	94.2:5.8	16.2(4)
108.9	1.2×10^{-4}	93.7:6.3	14.9(4)
113.6	1.8×10^{-4}	93.1:6.9	13.5(5)
122.8	4.6×10^{-4}	92.7:7.3	12.7(5)

[a] Data obtained from the equilibration experiment described in Figure 1. It does not fit on the van't Hoff plot since excess BINOL H-bonds to the product and perturbs the equilibrium.[33]

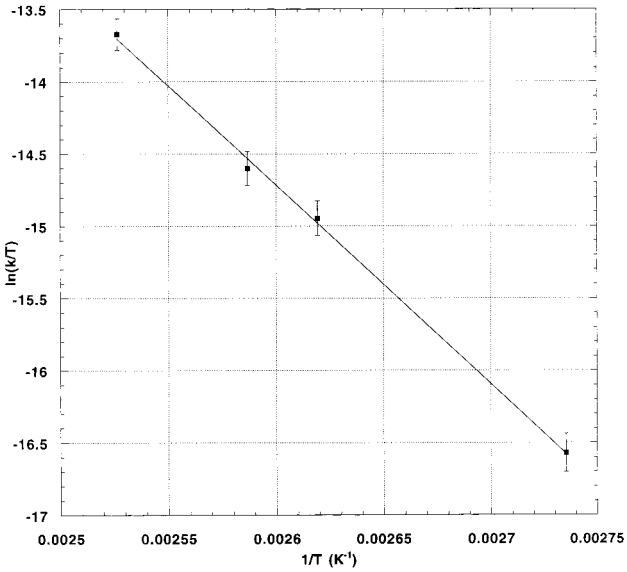

Figure 2. Eyring analysis for the thermal conversion of $\lambda(S)$-**5b** to $\delta(S)$-**5a**.

(12) Since biphenyl atropisomerism does not occur under these conditions, $\delta(S)$-**5a**, which is already the favored isomer, does not appreciably react with (*R*)-BINOL. Equations 8 and 9 thus only describe one set of reacting enantiomers.

(13) Since adventitious traces of ligand in racemic complexes could catalyze the isomerization through ligand exchange, only enantiopure diastereomers were studied.

(14) Errors are reported at the 95% confidence level (3σ), assuming a 10% margin of error on each rate constant, and were calculated by a nonlinear least-squares method; computer program kindly provided by Prof. Barry Carpenter of Cornell.

Table 3. Crystallographic Data for(±)-4a and λ(*S*)-5b

	(±)-**4a**·H_2O·$(C_2H_5)_2O$	λ(*S*)-**5b**·$3CH_2Cl_2$
empirical formula	$PtP_2SC_{51}H_{40}F_3NO_3$·$H_2O$·$(C_2H_5)_2O$	$PtP_2C_{56}H_{40}O_2$·$3CH_2Cl_2$
fw	1083.99	1255.75
space group	orthorhombic *Pcab* (61)	orthorhombic $P2_12_12_1$ (19)
a	19.1768(8)	15.6986(5)
b	24.0196(10)	15.7021(5)
c	41.0509(16)	21.2205(6)
V, Å^3	18908.8(13)	5230.9(3)
Z	16	4
T, °C	−100	−100
D_c, g/cm^3	1.523	1.595
λ, Å	Mo Kα (0.71073)	Mo Kα (0.71073)
μ, nm^{-1}	3.12	3.08
R_f[a]	0.042	0.023
R_w[b]	0.062	0.027
GOF[c]	2.6596	1.1986

[a] $R_f = \sum(F_o - F_c)/\sum F_o$. [b] $R_w = [\sum w(F_o - F_c)^2/\sum wF_o^2]^{1/2}$. [c] GOF = $[\sum w(F_o - F_c)^2/(n - p)]^{1/2}$, where n = number of reflections and p = number of parameters.

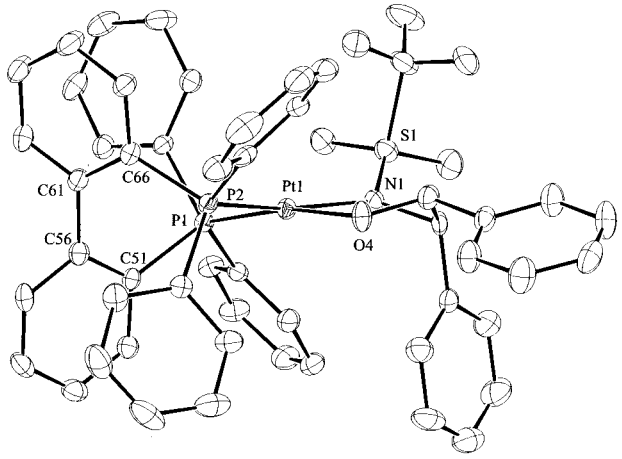

Figure 3. ORTEP representation of the X-ray structure of (±)-**4a**, (λ(1*S*,2*R*) shown). Thermal ellipsoids are at the 50% probability level. Selected bond distances (Å) and bond angles (deg): Pt−P1 = 2.2505(18), Pt−P2 = 2.2380(19), Pt−N1 = 2.094(6), Pt−O4 = 2.024(5), P1−Pt−P2 = 93.03-(7), O1−Pt−N1 = 81.25(21), P2−Pt−O4 = 87.45(15), P1−Pt−N4 = 99.55(17), C51−C56−C61−C66 = 65.1(10).

high thermodynamic selectivity observed for the combination of a single chiral ligand and a single biphep skew conformation, X-ray structures of (±)-**4a** and λ(*S*)-**5b** were obtained. Acquisition and structure refinement parameters are collected in Table 3; complete tables of metrical parameters are available in the Supporting Information. (±)-**4a** crystallizes into a centrosymmetric space group with two independent, but nearly identical molecules in the asymmetric unit. As indicated in Figure 3 for an arbitrary molecule, the structure of the major isomer corresponds to **4a**. The biphep portion of the molecule is unexceptional and looks like many BINAP[15] and a recent biphep$PdCl_2$[16] structure with a biphenyl dihedral angle of 65.1(10)°. Torsional strain in the seven-membered chelate causes the biphep ligand to skew relative to the P−Pt−P plane (C61−C56 vector is angled 63° to the P−Pt−P plane). The N−Pt−O plane is distorted 13° relative to the P−Pt−P plane and toward the pseudoaxial P−Phs. The triflamide portion of **4a** is similar to this fragment coordinated to dppePt[8] and is characterized by an axial phenyl substituent α to the nitrogen ligand and an equatorial phenyl group α to oxygen. These orientations are apparently also maintained in solution, as $^3J_{Pt-H}$ coupling to the pseudoaxial H on the carbinol carbon is small, while $^3J_{Pt-H}$ for the pseudoequatorial H on the center α to N is large (36 Hz). A Karplus-like relationship correlating $^3J_{Pt-H}$ to the Pt−X−C−H dihedral has been noted.[17]

The sterically dominant group in the O,NTf chiral ligand is the SO_2 moiety, as one oxygen protrudes into the open quadrant created by one of the back pointing pseudoaxial P-phenyl substituents. The thermodynamic selectivity for the major isomer is readily understood by considering that the biphep atropisomer would position a sterically dominant pseudoequatorial P−Ph into this same quadrant. The major isomer thus efficiently gears the SO_2 portion and the protruding pseudoequatorial P−Ph.

Unlike **4a**, λ(*S*)-**5b** is the thermodynamically less favored diastereomer and represents the "mismatched" combination of biphep and BINOL stereochemistries. In addition to confirming the relative stereochemistry of the biphep and BINOL fragments, the mismatched Pt−BINOL complex λ(*S*)-**5b** also has an unusual solid-state structure (Figure 4A).[18] In particular, the structure does not have C_2-symmetry, as the biphep ligand is highly distorted above the square plane in an effort to minimize the interaction between its forward pointing pseudoequatorial P−Ph groups and the 3,3′-C−H's of BINOL; that is, both attempt to occupy the same quadrants. To minimize this interaction, the structure skews the biphenyl backbone so that one-half of biphep has two P−Ph substituents roughly evenly disposed about the square plane (neutral axial/equatorial designations) while the other half has overemphasized the axial/equatorial positions to such an extent that one P−Ph almost lies in the square plane while the other is pulled well back. Most illustrative of this P−Ph skewing are the P−Pt−P−C_{ipso} dihedral angles expressed as rotations above and below the P−Pt−P square plane (Figure 4B). In the more "symmetric" half of the molecule, P−Ph(23) is rotated 73.8° above the plane while P−Ph-(29) is rotated 44° below. In contrast, the more "distorted" phosphine has P−Ph(53) and P−Ph(47) rotated 6.2° above and 113° below the plane, respectively. The sum of these dihedral angles is similar for each phosphorus, 117.8 and 119.2°, respectively, indicating that the axial/equatorial distortions are primarily torsional in nature. In addition to twisting, there is also significant bond distance and angle variability in the structure. In particular, P(1)−Pt−O(22) (85.60(5)°) is significantly more acute than P(2)−Pt−O(1) (95.70(5)°), though

(15) Ohta, T.; Takaya, H.; Noyori, R. *Inorg. Chem.* **1988**, *27*, 566−569.

(16) Ogasawara, M.; Yoshida, K.; Hayashi, T. *Organometallics* **2000**, *19*, 1567−1571.

(17) (a) Cerasino, L.; Williams, K. M.; Intini, F. P.; Cini, R.; Marzilli, L. G.; Natile, G. *Inorg. Chem.* **1997**, *36*, 6070−6079. (b) Appleton, T. G.; Hall, J. R. *Inorg. Chem.* **1971**, *10*, 1717−1725. (c) Erickson, L. E.; McDonald, J. W.; Howie, J. K.; Clow, R. P. *J. Am. Chem. Soc.* **1968**, *90*, 6371−6382. (d) Yano, S.; Tukada, T.; Saburi, M.; Yoshikawa, S. *Inorg. Chem.* **1978**, *17*, 2520−2526. (e) Erickson, L. E.; Sarneski, J. E.; Reilley, C. N. *Inorg. Chem.* **1975**, *14*, 3007−3017.

(18) For other examples of unusual BINOL structures as a consequence of stereochemical mismatching, see: (a) Brunkan, N. M.; White, P. S.; Gagné, M. R. *Angew. Chem., Int. Ed.* **1998**, *37*, 1579−1582. (b) Brunkan, N. M.; White, P. S.; Gagné, M. R. *J. Am. Chem. Soc.* **1998**, *120*, 11002−11003.

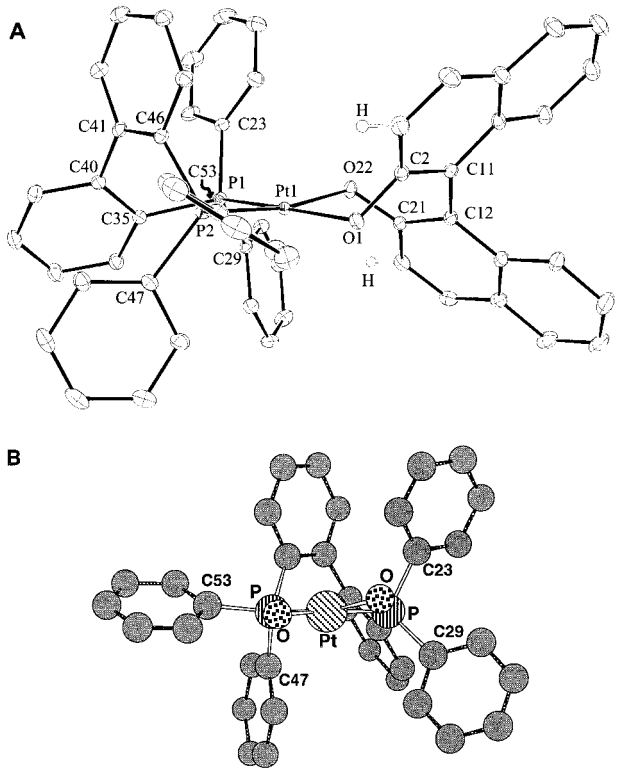

Figure 4. (A) ORTEP representation of $\lambda(S)$-**5b** (thermal ellipsoids at the 50% probability level). Selected bond distance (Å) and angles (deg) not discussed in the text: P(1)−Pt−P(2) = 91.456(24), O(1)−Pt−O(22) = 87.67(7). (B) Chem3D picture highlighting the biphep distortion. The non-oxygen-containing fragment of BINOL is removed for clarity.

Scheme 2

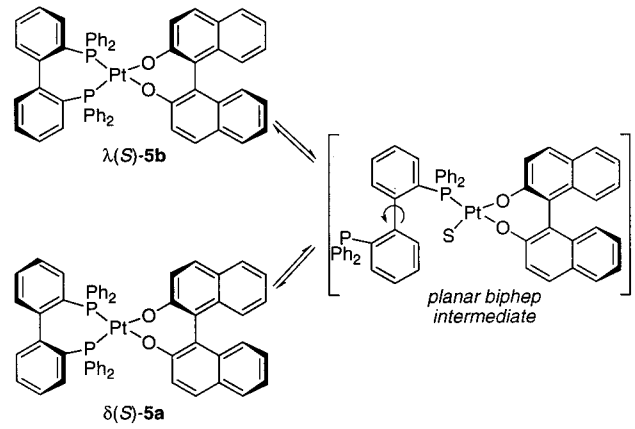

Scheme 3

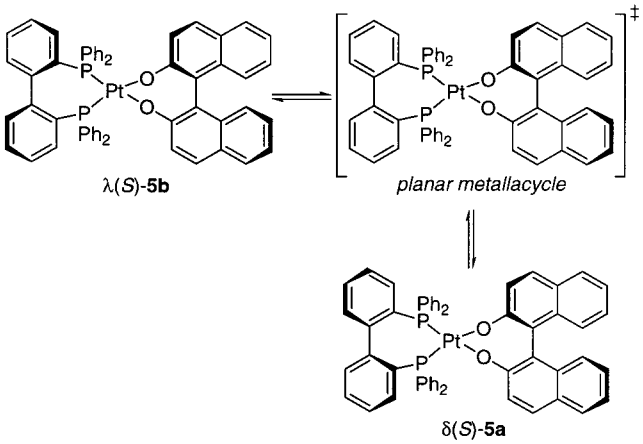

the P(1)−Pt (2.2368(6)) and O(22)−Pt (2.0706(17)) bond distances (Å) are longer than those on the "distorted" side of the molecule (2.2180(7) and 2.0353(17) Å, respectively). The biphep and BINOL dihedral angles describing the atrop-isomerism are 63.4(4)° and 57.8(4)°, respectively, and the O−Pt−O plane is distorted 10° from the P−Pt−P plane and toward the pseudoaxial P−Ph substituents (counterclockwise). Since a singlet is observed in the ^{31}P NMR, the structural distortions must be either time averaged or unique to the solid state. The $\delta(S)$-**5a** diastereomer is presumably thermodynamically favored because the BINOL projects its 3,3′-positions toward the less congested P−Ph pseudoaxial positions.[19,20]

(6) Mechanistic Possibilities. Chiral ligand additive studies (section 3) showed that ligand−ligand exchange with enantiomeric ligands was the most rapid mechanism for diastereomer interconversion and that biphep stereoinversion was not competitive. However, since enantiopure X_2 ligand exchange processes cannot be responsible for the thermal isomerization of $\lambda(S)$-**5b** to $\delta(S)$-**5a** (∼94:6) (section 4), this requires net biphep atrop-inversion by a second mechanism. As noted by Mikami and Noyori for octahedral Ru complexes,[1] two reasonable but kinetically indistinguishable mechanisms are possible, both of which also apply to biphep-PtX$_2$: dissociation induced biaryl rotation (Scheme 2), and on-metal concerted inversion (Scheme 3). Both mechanisms have weak points, though, as the dissociative pathway breaks a strong P−Pt bond to generate a three-coordinate PPtX$_2$ intermediate (with or without solvent coordination), and the on-metal skew inversion proceeds through a strained planar seven-membered metallacycle containing two long P−Pt bonds and four sp^2 centers.

The large difference in rate between biphepRu(NN)Cl$_2$ ($t_{1/2}$ 10's of min at 25 °C) and the biphepPtX$_2$ complexes ($t_{1/2}$ of hours at 100 °C) is most easily reconciled with a dissociative mechanism that is facile with 18-electron octahedral Ru(II) complexes[21] and attenuated with substitution-inert biphepPtX$_2$ complexes (Scheme 2). Since preequilibrium dissociation of a chelated diphosphine arm is documented in dppePtMe$_4$ reductive elimination (165−200 °C),[22] similar phosphine dissociation-induced reactivity may be operative in biphepPtX$_2$ complexes; the elevated isomerization

(19) BINOL also strongly affects the relative energetics of the biphenyl atropisomers in Brintzinger's biphenylCp$_2$Ti(BINOL) complexes; see ref 20.

(20) Ringwald, M.; Stürmer, R.; Brintzinger, H. H. *J. Am. Chem. Soc.* **1999**, *121*, 1524−1527.

(21) (PPh$_3$)$_4$RuCl$_2$ is known to be extensively dissociated in solution, giving rise to the 14- and 16-electron complexes, (PPh$_3$)$_2$RuCl$_2$ and (PPh$_3$)$_3$RuCl$_2$, respectively. (a) Caulton, K. G. *J. Am. Chem. Soc.* **1974**, *96*, 3005−3006. (b) James, B. R.; Markham, L. D. *Inorg. Chem.* **1974**, *13*, 97−100. Substitution of water from [Ru^{II}(OH$_2$)(bpy)$_2$(PR$_3$)]$^{2+}$ by incoming ligands is also known to be dissociation initiated; see: Leising, R. A.; Ohman, J. S.; Takeuchi, K. J. *Inorg. Chem.* **1988**, *27*, 3804−3809. For a general discourse on substitution mechanisms of octahedral organometallic complexes, see: (c) Atwood, J. D. *Inorganic and Organometallic Reaction Mechanisms*, 2nd ed.; VCH Publishers: New York, 1997.

(22) Crumpton, D. M.; Goldberg, K. I. *J. Am. Chem. Soc.* **2000**, *122*, 962−963.

Scheme 4

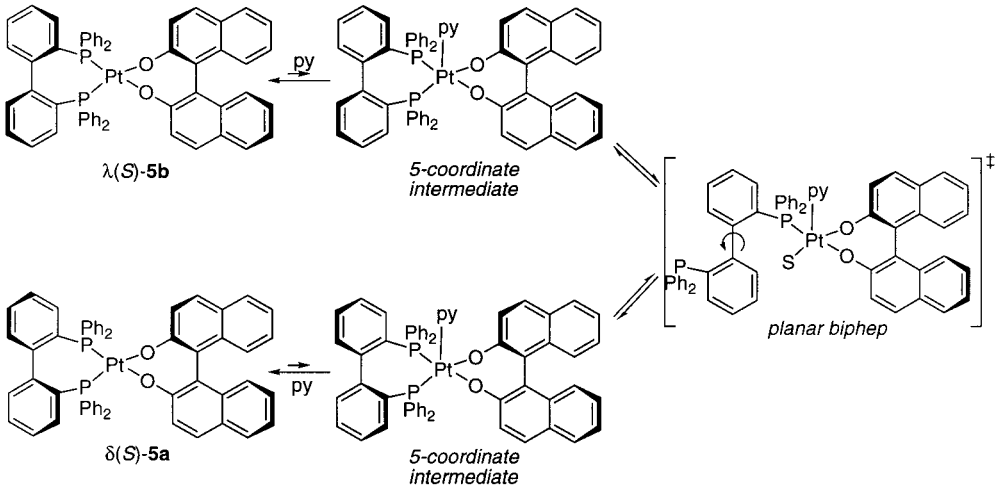

temperatures are consistent with an expectedly slow initiating P−Pt bond breakage.

A dissociative radical mechanism has been proposed in a conceptually similar thermal isomerization (60−110 °C) of biphenyl-linked metallocene BINOL complexes (**A**, M = Ti, Zr). Stable free radical additives such as TEMPO were observed to accelerate the isomerization rate, presumably via a dechelated cyclopentadienyl radical.[20]

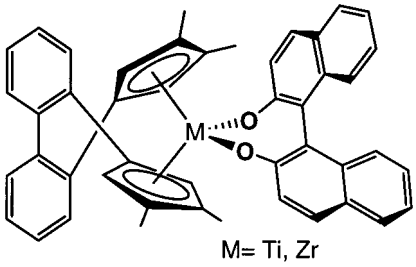

A

The on-metal atrop-inversion process, however, cannot be dismissed (Scheme 3). In particular, the rapid atrop-isomerism observed in 2,2′-diamino-1,1′-biphenyl complexes of Ru and Os (millisecond time scale), known to rigorously proceed by a concerted mechanism, **B**, suggests that the planar biphep transition state might be feasible.[23,24] Most problematic in assessing the importance of this mechanism is rationalizing the large difference in rate observed for biphenyldiamine complexes, **B** ($t_{1/2}$ ∼100 ms, 25 °C), the diphosphine complexes biphepRu(NN)Cl_2 ($t_{1/2}$ ∼20 min, 25 °C), and biphepPt(BINOL) ($t_{1/2}$ 8.5 h, 90 °C). Since substituting NH_2 for PPh_2 increases the M−X bond lengths (X = N, P),[25] this change might add additional strain to the cyclic transition state and slow the biphep systems

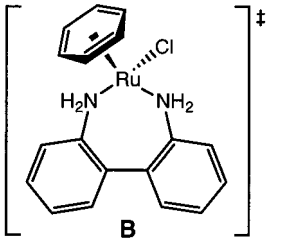

B

relative to the diamine. Moreover, if ring strain in the planar biphep transition state was attenuated by lengthening the P−Ru and P−Pt bonds (with concomitant compression of P−M−P bond angles), then the energetic cost for such a distortion would depend on the absolute ground-state bond strengths (P−Ru < P−Pt)[26] and the plasticity of the P−M−P bond angle. In this scenario partial breakage of the P−Ru and P−Pt bonds occurs en route to the transition state, the energetic cost of which is regained on the return to products. Arguing against any significant breakage in at least the diamine case, however, is the modest rate decrease (∼2×) on substituting Ru for Os in **B**. Another possibility for explaining the Ru > Pt rate ordering points to the axial chloride ligands in biphepRu(NN)Cl_2. If these ligands buttress the pseudoaxial P−Ph groups sufficiently to raise the ground state energy, then reduction of this interaction in the transition state would lead to an overall rate enhancement relative to a square-planar coordination environment, all things being equal. Steric effects on the rate of biphep atrop-inversion however must be interpreted cautiously, as the barrier is known to be variable and sensitive to substitution in simple constrained biaryl compounds such as **C**−**F**, more rigid, substituted backbones tending toward higher activation energies.[27] Since the available data do not distinguish between the two proposed mechanisms for biaryl atrop-inversion (the activation parameters are not helpful), a mechanism for the thermal isomerization of diastereomers cannot be assigned at this time. Future studies

(23) (a) Alguindigue, S. S.; Khan, M. A.; Ashby, M. T. *Organometallics* **1999**, *18*, 5112−5119. Similarly, 1,1′-biisoquinoline derivatives of Ru and Os are known to rigorously undergo atrop-inversion by a chelated transition state. (b) Ashby, M. T.; Govindan, G. N.; Grafton, A. K. *J. Am. Chem. Soc.* **1994**, *116*, 4801−4809. (c) Ashby, M. T. *J. Am. Chem. Soc.* **1995**, *117*, 2000−2007. (d) Ashby, M. T.; Alguindigue, S. S.; Khan, M. A. *Organometallics* **2000**, *19*, 547−552.

(24) Phosphite ligands based on 2,2′-biphenol are also known to rapidly invert their atropisomers while coordinated to Mo and Pt; see: Hariharasarma, M.; Lake, C. M.; Watkins, C. L.; Gray, G. M. *Organometallics* **1999**, *18*, 2593−2600.

(25) Ru−N bond lengths in (C_6H_6)RuCl(2,2′-diamino-1,1′-biphenyl) are 2.172(6) Å; cf. the Pt−P bond lengths of ∼2.24 Å observed herein.

(26) (a) Li, C.; Cucullu, M. E.; McIntyre, R. A.; Stevens, E. D.; Nolan, S. P. *Organometallics* **1994**, *13*, 3621−3627. (b) Haar, C. M.; Nolan, S. P.; Marshall, W. J.; Moloy, K. G. *Organometallics* **1999**, *18*, 474−479.

(27) This argument was originally put forth by Ashby and coworkers; see footnote 23a and references therein.

examining Pd analogues might shed additional light on the subject.

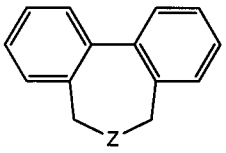

		$\Delta G^{\ddagger}$(kcal mol^{-1})
C:	Z= O	9
D:	Z = S	17
E:	Z = CH_2	12
F:	Z = $C(CO_2H)_2$	23

Since square-planar Pt(II) complexes tend to react via associative mechanisms, we reasoned that donor ligands might catalyze the isomerization by increasing the dissociation rate of a phosphine arm from a five-coordinate intermediate (Scheme 4). Indeed, $\lambda(S)$-**5b** is gradually converted to the thermodynamically preferred $\delta(S)$-**5a** isomer (95:5) with gentle warming in pyridine (24 h at 40 °C). This corresponds to a reduction in the isomerization temperature of 60−70 °C.[28] Moreover, this decrease in temperature allowed a ∼1:1 mixture of $\delta(1R,2S)$-**4a** and $\lambda(1R,2S)$-**4b** to be converted to $\delta(1R,2S)$-**4a** (>97:3) at 52 °C; thermolysis in toluene (100 °C) leads to extensive decomposition. While the arm-off mechanism is reasonable for the pyridine-catalyzed reaction, it is not clear whether this represents an accelerated arm-off mechanism or a new mechanism that operates at low temperatures; that is, pyridine catalysis does not necessarily shed light on the noncatalyzed process.

(7) Summary. Examination of diastereomer interconversion processes in biphepPtX$_2$ complexes revealed that at least three mechanisms are available. In the presence of enantiomeric chiral X_2 ligands, the data clearly indicate that X_2-X_2 ligand exchange processes dominate the isomerization kinetics and that biphep stereoinversion is not competitive. On the other hand, when the X_2 ligand is enantiopure, X_2-X_2 ligand exchange is unproductive and higher energy processes are detected. Thermolysis of the minor biphepPtBINOL diastereomer (92−122 °C) in chlorobenzene leads to a thermodynamic mixture (∼94:6) by a mechanism that requires biphep biaryl rotation and atrop-inversion of the diphosphine stereochemistry. Two mechanisms are consistent with the data: on-metal inversion through a planar seven-membered transition state, and one-arm-off prior to rotation. The isomerization kinetics of the enantiopure ligand systems could be substantially accelerated with pyridine in a process that is proposed to involve a five-coordinate pyridine adduct (undetected), which has a higher phosphine dissociation rate than in the square-planar complex (or the on-metal stereoinversion rate).

Regardless of the microscopic details of the process that leads to biaryl rotation and atrop-inversion, it is clear that the diphosphine stereochemistry in substitution-inert biphepPtX$_2$ complexes is kinetically more robust than the octahedral biphepRu(NN)Cl$_2$ catalyst reported by Mikami and Noyori.

Experimental Section

General Comments. (cod)PtCl$_2$ was prepared according to literature protocol.[29] ^{1}H, ^{13}C, ^{13}C{^{31}P}, and ^{31}P NMR spectra were recorded at ambient temperatures on a Bruker AMX300 or AMX400 spectrometer (300 or 400 MHz, ^{1}H, respectively). ^{31}P NMR spectra were obtained using 85% H_3PO_4 as an external reference. All solvents but THF were purified by passing over activated alumina columns,[30] and THF was dried over Na-benzophenone ketyl. Optical rotation measurements were obtained on a Jasco DIP-1000 digital polarimeter. Elemental analyses were performed by E+R Microanalytical Laboratory, Inc. (Parsippany, NJ).

Biphep. To a flame-dried flask was added 4.0 g (14.4 mmol) of triphenylphosphine oxide under nitrogen. The solid was dissolved in 140 mL of THF and cooled to −78 °C, and then 1.05 equiv (15.1 mmol) of freshly titrated *sec*-butyllithium was slowly added. The deep red homogeneous solution was stirred at −78 °C for 3 h and then warmed to 0 °C. Copper(II) pivalate (43.1 mmol, 11.5 g) in 50 mL of THF was transferred via cannula to the triphenylphosphine oxide solution. After stirring for 4 h at 0 °C, the solvent was removed by rotary evaporation and the blue residue dissolved in a 3:1 solution of ethyl acetate/THF. The residual copper and lithium were extracted with a saturated ammonium chloride solution (2 × 100 mL) and a saturated sodium bicarbonate solution (4 × 100 mL) until the organic layer was colorless. The organic layer was washed with brine (2 × 100 mL), dried over magnesium sulfate, and filtered. After solvent was removed by rotary evaporation, the crude biphep oxide was dried in vacuo and dissolved in 90 mL of xylenes. To the stirring solution was added 3.4 mL of triethylamine (2.38 g, 23.5 mmol) and 2.86 mL of trichlorosilane (3.23 g, 28.7 mmol, 4 equiv). The solution was heated at 100, 120, and 140 °C, each for 1 h. After cooling to 50 °C, 45 mL of 30% NaOH was added slowly. The layers were separated, and the NaOH layer was extracted with 30 mL of toluene. To the combined organic fractions was added 45 mL of 30% NaOH, and the mixture was vigorously shaken. The aqueous layer was removed and back extracted with toluene (2 × 60 mL). The organic layers were combined, washed with brine (2 × 100 mL), and dried over $MgSO_4$, and the solvent was removed by rotary evaporation. The crude mixture was recrystallized from 1:3 toluene/ethanol to afford crystals of biphep in an overall 30% yield. ^{31}P NMR (121.5 MHz, CD_2Cl_2): δ −13.7. ^{1}H NMR (300.1 MHz, CD_2Cl_2): δ 7.24 (m, 24 H), 7.07 (br d, 2H, J = 9 Hz), 6.89 (br d, 2H, J = 9 Hz). ^{13}C{^{31}P} NMR (75.5 MHz, CD_2Cl_2): δ 147.7, 138.4, 137.7, 137.0, 134.2, 133.8, 131.2, 128.8, 128.6, 128.5, 128.4, 128.0.[31] Anal. Calcd for $C_{36}H_{28}P_2$; C, 82.74; H, 5.40. Found: C, 82.77; H, 5.71.

(biphep)PtCl$_2$ (1). To a stirring solution of 358.5 mg (0.958 mmol, 1 equiv) of (cod)PtCl$_2$ in 35 mL of CH_2Cl_2 was added dropwise 499.9 mg (0.956 mmol, 1 equiv) of biphep in 35 mL of CH_2Cl_2. After 10 min of stirring, the solvent was removed and the white powder was recrystallized in CH_2Cl_2/MeOH, producing 685 mg of white crystals (90% yield). ^{31}P NMR (121.5 MHz, CD_2Cl_2): δ 7.9 (J_{P-Pt} = 3610 Hz). ^{1}H NMR (300.1 MHz, CD_2Cl_2): δ 7.74 (4H, q, J = 9 Hz), 7.6 (4H, m), 7.4 (8H, m), 7.2 (4H, t, J = 9 Hz), 7.0 (6H, m), 6.65 (2H, dd, J = 9, 6 Hz). ^{13}C{^{31}P} (75.5 MHz, CD_2Cl_2): δ 144.0, 136.1, 135.5, 134.0, 133.2, 132.1, 131.9, 131.3, 128.7, 128.2, 128.1, 128.0, 127.8, 124.8. Anal. Calcd for $C_{36}H_{28}P_2PtCl_2 \cdot CH_2Cl_2$: C, 50.90; H, 3.47. Found: C, 50.82; H, 3.47.

(biphep)PtCO$_3$ (2). To a solution of 300 mg (0.380 mmol, 1 equiv) of **1** in 40 mL of wet CH_2Cl_2 was added silver carbonate (190 mg, 0.689 mmol, 1.8 equiv) in 20 mL of wet CH_2Cl_2. The mixture was stirred in darkness for 3 h and then filtered through Celite to remove the AgCl. **2** was precipitated from solution using hexanes and was recrystallized CH_2Cl_2/

(28) Monodentate phosphines such as PPh_3, P(2-MePh)$_3$, PBu_3, $P(OMe)_3$, $P(OPh)_3$, PMe_3, excess biphep, and other donor solvents such as DMSO, DMF, THF, and CH_3CN either did not affect the rate of BINOLate diastereomer interconversion or led to decomposition.

(29) (a) Slack, D. A.; Baird, M. C. *Inorg. Chim. Acta* **1977**, *24*, 277. (b) McDermott, J. X.; Whitesides, G. M. *J. Am. Chem. Soc.* **1976**, *98*, 6521.

(30) Pangborn, A. B.; Giardello, M. A.; Grubbs, R. H.; Rosen, R. K.; Timmers, F. *Organometallics* **1996**, *15*, 1518−1520.

(31) Not all ^{13}C resonances were located.

hexanes to afford 248 mg of the pale yellow solid (84% yield). ^{31}P NMR (162.0 MHz, CD_2Cl_2): δ 2.2 (J_{P-Pt} = 3570 Hz). ^{1}H NMR (400.1 MHz, CD_2Cl_2): δ 7.7 (8H, m), 7.5 (6H, m), 7.3 (2H, t, J = 8 Hz), 7.2 (4H, t, J = 8 Hz), 7.1 (2H, t, J = 8 Hz), 7.0 (2H, d, J = 8 Hz), 6.8 (4H, m). ^{13}C{^{31}P} (75.5 MHz, CD_2Cl_2): δ 143.8, 135.2, 135.0, 134.9, 134.0, 132.2, 132.0, 131.9, 131.8, 128.8, 128.6, 128.1, 127.4, 126.0, 125.6. Anal. Calcd for $C_{37}H_{28}P_2PtO_3$: C, 57.15; H, 3.63. Found: C, 56.92; H, 3.52.

(biphep)Pt(1*R*,2*S*)-TfNO (δ(1*R*,2*S*)-4a, λ(1*R*,2*S*)-4b). A 100 mg sample of **2** (0.128 mmol) and 44.4 mg (0.128 mmol) of (1*R*,2*S*)-**3** were dissolved in 5 mL of CH_2Cl_2 and stirred at room temperature for 1 h. The solvent was removed and the white solid dissolved in a minimum amount of CH_2Cl_2 and precipitated using hexanes to produce a ~1:1 mixture of diastereomers. The 1:1 ratio of δ(1*R*,2*S*)-**4a**:λ(1*R*,2*S*)-**4b** was recrystallized from CH_2Cl_2/hexanes to yield a colorless solid in 40% yield. A racemate of this mixture that was stable to isomerization could only be obtained if a deficiency of (±)-**3** (0.9 equiv) was used. Employing 1.1 equiv of (±)-**3** led to (±)-**4a**, which was recrystallized from CH_2Cl_2/hexanes (47% yield).

(major, (±)-4a): ^{31}P NMR (162.0 MHz, CD_2Cl_2): δ 7.2 (d, $^1J_{Pt-P}$ = 3760 Hz, J_{P-P} = 31.3 Hz, trans to N), 3.5 (d, $^1J_{Pt-P}$ = 3210 Hz, J_{P-P} = 31.3 Hz, trans to O). ^{1}H NMR (300.1 MHz, CD_2Cl_2): δ 7.8 (m, 7H), 7.5 (m, 16 H), 7.0 (m, 12 H), 6.7 (m, 2 H), 6.4 (m, 1H), 5.4 (d, J = 6 Hz, C*H*O), 5.0 (br s, $^3J_{Pt-H}$ = 36 Hz, C*H*N). ^{13}C{^{31}P} (75.5 MHz, CD_2Cl_2): δ 144.9, 144.8, 143.2, 141.1, 135.3, 135.0, 134.0, 133.3, 132.2, 132.1, 131.9, 131.5, 131.2, 131.0, 130.9, 130.7, 130.2, 128.5, 128.0, 127.8, 127.7, 127.6, 127.5, 127.0, 126.7, 126.5, 126.0, 125.3, 125.0, 85.1 (*C*H), 71.5 (*C*H).[31] Anal. Calcd for $C_{51}H_{40}F_3NO_3P_2PtS$: C, 57.74; H, 3.80; N, 1.32. Found: C, 57.29; H, 3.84; N, 1.15. (**minor**, λ(1*R*,2*S*)-**4b**) could not be obtained free of the major isomer; characteristic resonances include the following. ^{31}P NMR (162.0 MHz, CD_2Cl_2): δ 8.9 (d, $^1J_{Pt-P}$ = 3725 Hz, J_{P-P} = 32.3 Hz, trans to *N*), 4.8 (d, $^1J_{Pt-P}$ = 3210 Hz, J_{P-P} = 32.3 Hz, trans to O). ^{1}H NMR (300.1 MHz, CD_2Cl_2): δ 5.6 (d, J = 6 Hz, C*H*O); 5.1 (br s, C*H*N, overlaps major diastereomer).

biphepPt(*S*)-BINOL (δ(*S*)-5a, λ(*S*)-5b). Method 1. A solution of sublimed NaOtBu (27.8 mg, 0.289 mmol) in 5 mL of THF was transferred via cannula to 40.9 mg (0.143 mmol) of (*S*)-BINOL in 5 mL of THF. This solution of Na_2BINOL was transferred via cannula to a slurry of **1** (112.9 mg, 0.143 mmol) in dry toluene. The yellow mixture became clear and yellow within 30 min, signifying completion of the reaction. The toluene was removed in vacuo, and the yellow solid triterated twice with 5 mL of dry toluene to remove residual *tert*-butyl alcohol. CH_2Cl_2 (10 mL) was added and the solution filtered to remove the NaCl byproduct. The product was precipitated from the supernatant in a 1:1 ratio of diastereomers using hexanes. A yellow solid that was ~1:1 δ(*S*)-**5a**/λ(*S*)-**5b** was isolated in 87% yield. Thermolysis of the latter complexes in toluene (90 °C) over 3 days provided δ(*S*)-**5a** (95:5). A mixture of racemic diastereomers could be obtained using racemic BINOL, though this material tended to isomerize, at a rate dependent on the concentration of free BINOL.

Method 2. **2** (24.4 mg, 0.031 mmol) and BINOL (either racemic or enantiomerically pure) (9.0 mg, 0.031 mmol) were dissolved in 0.5 mL of CD_2Cl_2, and the reaction was monitored by ^{31}P NMR. The reaction with *S*-BINOL took 5 days to complete at room temperature (1:1 mixture of diastereomers); the racemic BINOL reaction took 24 h and precipitated a 95:5 mixture of (±)**5a**/**5b** from solution. This solid was collected and recrystallized from chlorobenzene and hexanes in 91% yield.

(**major**, δ(*S*)-**5a**): ^{31}P NMR (162 MHz, CD_2Cl_2): δ 2.86 (J_{P-Pt} = 3670 Hz). ^{1}H NMR (400 Hz, CD_2Cl_2): δ 7.81 (m, 4 H), 7.72 (d, J = 7.7 Hz, 2 H), 7.59 (m, 4 H), 7.52 (d, J = 8.7 Hz, 2 H), 7.39 (m, 4 H), 7.26 (m, 8 H), 7.12 (m, 2 H), 7.01 (m, 4 H), 6.92 (t, J = 7.7 Hz, 2 H), 6.85 (d, J = 8.7 Hz, 4 H), 6.72 (d, J = 8.7 Hz, 2 H), 6.63 (m, 2 H). ^{13}C{^{31}P} NMR (75 MHz, CD_2Cl_2): δ 161.3, 143.8, 135.9, 135.7, 135.3, 134.0, 132.1, 131.8, 131.4, 131.2, 128.9, 128.7, 128.5, 128.1, 127.9, 127.8, 127.3, 126.0, 125.8, 125.7, 124.9, 124.7, 122.8, 121.2. $[\alpha]_D^{26.1} = -138.1$ (*c* 0.605 in ClC_6H_5, contains 5% λ(*S*)-**5b**). Anal. Calcd for $C_{56}H_{40}P_2PtO_2$: C, 67.13; H, 4.02. Found: C, 66.9; H, 4.0. (**minor**, λ(*S*)-**5b**): ^{31}P NMR (162 MHz, CD_2Cl_2): δ 2.64 (J_{P-Pt} = 3643 Hz). ^{1}H NMR (400 Hz, CD_2Cl_2): δ 8.04 (m, 4 H), 7.70 (d, J = 8.1 Hz, 2 H), 7.53 (m, 12 H), 7.28 (m, 2 H), 7.09 (m, 8 H), 6.98 (t, J = 8.3 Hz, 2 H), 6.88 (t, J = 8.6 Hz, 6 H), 6.76 (m, 2 H), 6.23 (d, J = 8.8 Hz, 2 H). ^{13}C{^{31}P} NMR (75 MHz, CD_2Cl_2): δ 161.5, 143.5, 135.5, 134.8, 134.5, 133.1, 132.7, 131.6, 131.2, 130.9, 128.9, 128.8, 128.3, 128.2, 127.9, 127.8, 127.4, 125.4, 125.2, 124.7, 124.1, 121.3.[31] $[\alpha]_D^{26.1} = 36.7$ (*c* 0.610 in ClC_6H_5). Anal. Calcd for $C_{56}H_{40}P_2PtO_2 \cdot 2CH_2Cl_2$: C, 59.45; H, 3.78. Found: C, 59.48; H, 4.02.

Ligand Exchange Kinetics. A typical procedure for the isomerization of λ(*S*)-**5b** to λ(*R*)-**5a** through ligand exchange is as follows. A 15 mg sample (15 μmol) of a 1:1 mixture of λ(*S*)-**5b** and δ(*S*)-**5a** was dissolved in 1.0 mL of chlorobenzene. One equivalent of (*R*)-BINOL (4.3 mg, 15 μmols) was added to the solution, and then it was transferred into an NMR tube containing a sealed benzene-d_6 capillary to provide a lock signal and immediately cooled (−78 °C). The sample was warmed and inserted into a preheated NMR probe (45 °C), and data collection was initiated; no diastereomer overlap occurred at 45 °C. Control experiments with 1 equiv of (*S*)-BINOL and no additive were carried out in parallel.

Thermolysis Kinetics. A typical procedure for the thermal isomerization of λ(*S*)-**5b** to δ(*S*)-**5a** is as follows. A solution of 6.2 mg (5.1 μmol) of λ(S)-**5b** in 0.8 mL of chlorobenzene was placed in an NMR tube containing a sealed capillary that was filled with benzene-d_6 to provide a lock signal. The solution was heated to 92.6 °C in an oil bath. After a known amount of time, the NMR tube was removed from the oil bath and immediately cooled to 0 °C to halt the thermal isomerization. The conversion to product was monitored by ^{31}P NMR at room temperature; the two diastereomers are overlapped at elevated temperature.

Crystallography. Crystals of (±)-**4a** suitable for X-ray crystallography were grown at room temperature from a saturated CH_2Cl_2 solution with slow diffusion of diethyl ether. Crystals of λ(*S*)-**5b** were grown from CD_2Cl_2 by slow evaporation. Single crystals were mounted in oil on the end of a fiber. Intensity data were collected on a Siemens SMART diffractometer with CCD detection using Mo Kα radiation of wavelength 0.710 73 Å (ω scan mode). The structures were solved by direct methods and refined by least-squares techniques on *F* using structure solution programs from the NARCVAX system.[32] All non-hydrogen atoms were refined anisotropically. Hydrogen atoms were placed in calculated positions (C−H = 0.96 Å) and allowed to ride on the atoms to which they were bonded. Crystal data, data collection, and refinement parameters are listed in Table 3. Absorption corrections were made using SADABS.

Acknowledgment. This research was partially supported by the NSF (CAREER, CHE-9624852), NIGMS (R01 GM60578-01), the Petroleum Research Fund, DuPont, and 3M. M.R.G. is a Camille Dreyfus Teacher Scholar (2000).

Supporting Information Available: Kinetic plots for the thermal isomerization of λ(*S*)-**5b** to δ(*S*)-**5a**, van't Hoff plot for the λ(*S*)-**5b** to δ(*S*)-**5a** equilibrium, kinetic plots for the isomerization of λ(1*R*,2*S*)-**4b** to λ(1*S*,2*R*)-**4a**, and complete tables of acquisition and metrical parameters for λ(*S*)-**5b** and (±)-**4a**. This material is available free of charge via the Internet at http://pubs.acs.org.

OM000629A

(32) Gabe, E. J.; Le Page, Y.; Charland, J. P.; Lee, F. L.; White, P. S. *J. Appl. Crystallogr.* **1989**, *22*, 384.
(33) Andrews, M. A.; Cook, G. K.; Shriver, Z. H. *Inorg. Chem.* **1997**, *36*, 5832−5844.